

## SUPPORTING INFORMATION

### **Toward novel sulphur-containing derivatives of tetraazacyclododecane: synthesis, acid-base properties, spectroscopic characterization, DFT calculations, and Cadmium(II) complex formation in aqueous solution**

Marianna Tosato,<sup>1</sup> Marco Verona,<sup>2</sup> Riccardo Doro,<sup>1</sup> Marco Dalla Tiezza,<sup>1</sup> Laura Orian,<sup>1</sup> Alberto Andrighetto,<sup>3</sup> Paolo Pastore,<sup>1</sup> Giovanni Marzaro,<sup>2</sup> Valerio Di Marco<sup>1,\*</sup>

<sup>1</sup> Department of Chemical Sciences, University of Padova, via Marzolo 1, 35131 Padova, Italy. email: [valerio.dimarco@unipd.it](mailto:valerio.dimarco@unipd.it)

<sup>2</sup> Department of Pharmaceutical Sciences, University of Padova, via Marzolo 8, 35131 Padova, Italy.

<sup>3</sup> Italian Institute of Nuclear Physics, Legnaro National Laboratories, Viale dell'Università 2, 35020 Legnaro (Padova), Italy.

## Calculation of the stability constant of the Na<sup>+</sup>-compound complexes

The comparison of the last pK<sub>a</sub> data for each compound, in the presence and in the absence of Na<sup>+</sup> 0.15 mol/L, allows to calculate the equilibrium constants ( $\beta_{\text{Na}}$ ) of the Na<sup>+</sup> complex, in the hypothesis that the latter has a 1:1 Na:compound stoichiometry and that Na<sup>+</sup> binds to the completely deprotonated form of the compound (A).

If pK<sub>a(Na)</sub> is the last pK<sub>a</sub> value obtained in the presence of Na<sup>+</sup>, and pK<sub>a(TMA)</sub> is the same value obtained without Na<sup>+</sup> (in the presence of TMA<sup>+</sup>), then their ratio represents the fraction of compound which is not bound to Na<sup>+</sup>:

$$\frac{\text{p}K_{\text{a(Na)}}}{\text{p}K_{\text{a(TMA)}}} = \frac{[\text{A}]}{[\text{A}] + [\text{NaA}]} \quad (1)$$

where NaA is the complex formed between A and Na<sup>+</sup>. If Na<sup>+</sup> is added as ionic strength buffer, its concentration is generally much larger than that of A. Under this condition, and if the Na<sup>+</sup> complex is not too weak, equation (2) can be replaced by:

$$\frac{\text{p}K_{\text{a(Na)}}}{\text{p}K_{\text{a(TMA)}}} \approx \frac{[\text{A}]}{[\text{NaA}]} \quad (2)$$

The mass balance for Na<sup>+</sup> is:

$$[\text{Na}^+] + [\text{NaA}] = C_{\text{Na}} \quad (3)$$

where C<sub>Na</sub> is the total Na<sup>+</sup> concentration (in our case 0.15 mol/L). As C<sub>Na</sub> is much larger than the total concentration of A, equation (3) becomes:

$$[\text{Na}^+] \approx C_{\text{Na}} \quad (4)$$

The formation constant of the sodium complex NaA,  $\beta_{\text{Na}}$ , is defined by equation (5):

$$\beta_{\text{Na}} = \frac{[\text{NaA}]}{[\text{A}][\text{Na}^+]} \quad (5)$$

By replacing equations (4) and (2) into equation (5), it results:

$$\beta_{\text{Na}} \approx \frac{\text{p}K_{\text{a(TMA)}}}{\text{p}K_{\text{a(Na)}} C_{\text{Na}}} \quad (6)$$

Table 1S. Electronic and Gibbs free energies (in gas-phase and in water) for nine conformers of cyclen. All the energies are in kcal mol<sup>-1</sup> and refer to the most stable structure (given in bold). Level of theory: (COSMO-)ZORA-OPBE/TZ2P//ZORA-OPBE/DZP. The infill of the circles denotes the position of the nitrogen atoms: a solid infill (black circle) indicates that the atoms are below the molecular plane; conversely, an empty infill indicates that the atoms are above the molecular plane. The cyclen conformer with two adjacent nitrogen atoms above the molecular plane (and the other two below the plane) with all four hydrogens inside the ring was not located on the potential energy surface (PES).

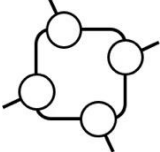
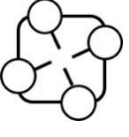
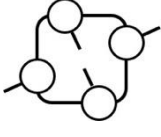
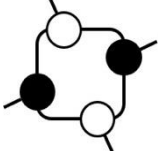
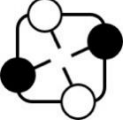
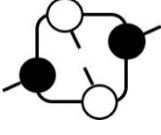
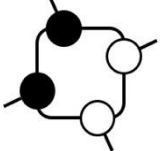
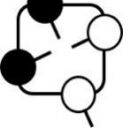
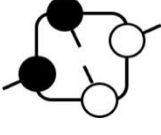
			
$\Delta E$	12.1	8.9	<b>0.0</b>
$\Delta E_{\text{H}_2\text{O}}$	7.0	5.8	<b>0.0</b>
$\Delta G$	9.8	8.4	<b>0.0</b>
$\Delta G_{\text{H}_2\text{O}}$	4.7	5.3	<b>0.0</b>
Point Group	C <sub>4</sub>	C <sub>2</sub>	<b>C<sub>2</sub></b>
			
$\Delta E$	10.0	13.9	4.2
$\Delta E_{\text{H}_2\text{O}}$	13.8	13.6	4.7
$\Delta G$	9.1	11.4	3.3
$\Delta G_{\text{H}_2\text{O}}$	13.0	11.2	3.8
Point Group	C <sub>2</sub>	C <sub>2</sub>	<b>C<sub>2</sub></b>
			
$\Delta E$	10.4	8.0	10.7
$\Delta E_{\text{H}_2\text{O}}$	9.9	8.2	9.9
$\Delta G$	9.4	6.7	9.4
$\Delta G_{\text{H}_2\text{O}}$	9.0	6.9	8.6
Point Group	C <sub>1</sub>	C <sub>1</sub>	<b>C<sub>1</sub></b>

Table 2S. Electronic and Gibbs free energies (in gas-phase and in water) for three monoprotonated and two bis-protonated conformers of cyclen. All the energies are in kcal mol<sup>-1</sup> and are relative to the most stable structure (in bold). Level of theory: (COSMO-)ZORA-OPBE/TZ2P//ZORA-OPBE/DZP.






			
$\Delta E$	<b>0.0</b>	11.5	-5.3
$\Delta E_{\text{H}_2\text{O}}$	<b>0.0</b>	9.8	2.3
$\Delta G$	<b>0.0</b>	10.6	-5.5
$\Delta G_{\text{H}_2\text{O}}$	<b>0.0</b>	8.9	2.0
Point Group	<b>C<sub>1</sub></b>	C <sub>1</sub>	C <sub>1</sub>
			
$\Delta E$	27.9	<b>0.0</b>	
$\Delta E_{\text{H}_2\text{O}}$	19.6	<b>0.0</b>	
$\Delta G$	26.3	<b>0.0</b>	
$\Delta G_{\text{H}_2\text{O}}$	18.1	<b>0.0</b>	
Point Group	C <sub>2</sub>	<b>C<sub>1</sub></b>	

Table 3S. Calculated pK<sub>a</sub> and  $\Delta G_{\text{H}_2\text{O}}$  (kcal mol<sup>-1</sup>) for cyclen. Level of theory: COSMO-ZORA-OPBE/TZ2P//ZORA-OPBE/DZP.

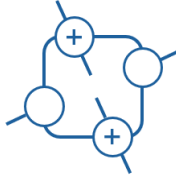
	$\text{pK}_{\text{a}3}$	$\Delta G_{\text{H}_2\text{O}}$	$\text{pK}_{\text{a}4}$	$\Delta G_{\text{H}_2\text{O}}$	$\Delta \text{pK}_{\text{a}}$
Method 1	9.0	12.2	11.5	15.7	2.5
Method 2	7.9	13.2	10.4	16.6	2.5

Table 4S. Calculated  $pK_a$  and  $\Delta G_{H_2O}$  (kcal mol<sup>-1</sup>) values for DO3S, paths A, B and C. Level of theory: COSMO-ZORA-OPBE/TZ2P//ZORA-OPBE/DZP.

path A					
	$pK_{a3}$	$\Delta G_{H_2O}$	$pK_{a4}$	$\Delta G_{H_2O}$	$\Delta pK_a$
Method 1	4.7	6.4	8.5	11.6	3.8
Method 2	3.7	7.4	7.5	12.6	3.8
path B					
	$pK_{a3}$	$\Delta G_{H_2O}$	$pK_{a4}$	$\Delta G_{H_2O}$	$\Delta pK_a$
Method 1	3.4	4.6	16.4	22.3	13.0
Method 2	2.3	5.5	15.3	23.3	13.0
path C					
	$pK_{a3}$	$\Delta G_{H_2O}$	$pK_{a4}$	$\Delta G_{H_2O}$	$\Delta pK_a$
Method 1	3.9	5.3	14.1	19.3	10.2
Method 2	2.9	6.3	13.1	20.2	10.2

Table 5S. Calculated  $pK_a$  and  $\Delta G_{H_2O}$  (kcal mol<sup>-1</sup>) for DO4S. Level of theory: COSMO-ZORA-OPBE/TZ2P//ZORA-OPBE/DZP.

	$pK_{a3}$	$\Delta G_{H_2O}$	$pK_{a4}$	$\Delta G_{H_2O}$	$\Delta pK_a$
Method 1	3.8	5.2	13.0	17.8	9.2
Method 2	2.8	6.1	12.0	18.7	9.2

Table 6S. <sup>1</sup>H-NMR signals of DO4S.  $\delta$  values (ppm) are given and the following information is reported in brackets: multiplicity, broadness (if applicable), area (if applicable), and proton assignment.

species	pD	<sup>1</sup> H-NMR signals
H <sub>2</sub> A <sup>2+</sup>	2.2, 3.2, 4.5, 6.8	2.20 (s, 12, SCH <sub>3</sub> ), 2.94 (m broad, 8, SCH <sub>2</sub> ), 3.28 (m broad, 24, NCH <sub>2</sub> )
H <sub>2</sub> A <sup>2+</sup> +HA <sup>+</sup>	7.7	2.19 (s, n.a., SCH <sub>3</sub> ), 2.8 (m broad, n.a., SCH <sub>2</sub> ), 2.9 (m broad, n.a., NCH <sub>2</sub> ring), 3.06 (m broad, n.a., NCH <sub>2</sub> arms), 3.29 (m broad, n.a., NCH <sub>2</sub> )
	8.5	2.18 (s, 12, SCH <sub>3</sub> ), 2.8 (m broad, 8, SCH <sub>2</sub> ), 2.9 (m broad, 16, NCH <sub>2</sub> ring), 3.06 (m broad, 8, NCH <sub>2</sub> arms)
HA <sup>+</sup>	9.8	2.17 (s, 12, SCH <sub>3</sub> ), 2.79 (t, 8, SCH <sub>2</sub> ), 2.88 (s, 16, NCH <sub>2</sub> ring), 3.04 (t, 8, NCH <sub>2</sub> arms)
HA <sup>+</sup> +A	10.8	2.17 (s, 12, SCH <sub>3</sub> ), 2.78 (t, 8, SCH <sub>2</sub> ), 2.87 (s, 16, NCH <sub>2</sub> ring), 3.01 (t, 8, NCH <sub>2</sub> arms)

Table 7S. <sup>1</sup>H-NMR signals of DO2A2S.  $\delta$  values (ppm) are given and the following information is reported in brackets: multiplicity, broadness (if applicable), area (if applicable), and proton assignment.

species	pD	<sup>1</sup> H-NMR signals
H <sub>3</sub> A <sup>+</sup>	2.5	2.16 (s, 6, SCH <sub>3</sub> ), 2.92 (t, 4, SCH <sub>2</sub> ), 3.07-3.25 (m broad, 8, NCH <sub>2</sub> ring close to sulfanyl arms), 3.45 (m broad, 8, NCH <sub>2</sub> ring close to acetate arms), 3.5 (t, 4, NCH <sub>2</sub> sulfanyl arms), 3.55 (s, 4, NCH <sub>2</sub> acetate arms)
	3.2	2.16 (s, 6, SCH <sub>3</sub> ), 2.89 (t broad, 4, SCH <sub>2</sub> ), 3.15-3.27 (m broad, 8, NCH <sub>2</sub> ring close to sulfanyl arms), 3.38 (m broad, 12, NCH <sub>2</sub> sulfanyl arms and NCH <sub>2</sub> ring close to acetate arms), 3.55 (s, 4, NCH <sub>2</sub> acetate arms)
H <sub>3</sub> A <sup>+</sup> +H <sub>2</sub> A	4.2	2.14 (s, 6, SCH <sub>3</sub> ), 2.80 (t broad, 4, SCH <sub>2</sub> ), 3.12 (s broad, 4, NCH <sub>2</sub> sulfanyl arms), 3.20 (s broad, 8, NCH <sub>2</sub> ring close to sulfanyl arms), 3.32 (s broad, 8, NCH <sub>2</sub> ring close to acetate arms), 3.63 (s broad, 4, NCH <sub>2</sub> acetate arms)
	5.0, 8.0, 9.1	2.14 (s, 6, SCH <sub>3</sub> ), 2.80 (t broad, 4, SCH <sub>2</sub> ), 3.10 (s broad, 4, NCH <sub>2</sub> sulfanyl arms), 3.15 (s broad, 8, NCH <sub>2</sub> ring close to sulfanyl arms), 3.35 (s broad, 8, NCH <sub>2</sub> ring close to acetate arms), 3.68 (s broad, 4, NCH <sub>2</sub> acetate arms)
H <sub>2</sub> A		
H <sub>2</sub> A+HA <sup>-</sup> +A <sup>2-</sup>	10.4	2.1-2.14 (m broad, 6, SCH <sub>3</sub> ), 2.60-3.10 (m broad, 24, SCH <sub>2</sub> , NCH <sub>2</sub> ring close to sulfanyl arms, NCH <sub>2</sub> ring close to acetate arms, and NCH <sub>2</sub> sulfanyl arms), 3.50 (s broad, 4, NCH <sub>2</sub> acetate arms)
H <sub>2</sub> A+HA <sup>-</sup> +A <sup>2-</sup>	11.8	2.1 (s, 6, SCH <sub>3</sub> ), 2.30-2.70 (m broad, 24, SCH <sub>2</sub> , NCH <sub>2</sub> ring close to sulfanyl arms, NCH <sub>2</sub> ring close to acetate arms, and NCH <sub>2</sub> sulfanyl arms), 3.10 (s broad, 4, NCH <sub>2</sub> acetate arms)

Table 8S. Lowest and most intense computed excitation energies (level of theory: COSMO-ZORA-SAOP/QZ4Pae//ZORA-OPBE/DZP) of cyclen, DO3S and DO4S.

		<b>COSMO-TD-DFT</b>	<b>Electronic transitions</b>
		<b>Values</b>	<b>[% assignment]</b>
<b>Cyclen</b>	<b>A</b>	5.5175 eV (0.0344) - 225 nm	HOMO→LUMO (98%)
		6.54765 eV (0.10040) - 200 nm	HOMO→LUMO+6 (96%)
	<b>HA<sup>+</sup></b>	5.6636 eV (0.00479) - 219 nm	HOMO→LUMO (99%)
		6.7329 eV (0.08054) - 184 nm	HOMO→LUMO+5 (85%)
	<b>H<sub>2</sub>A<sup>2+</sup></b>	6.1566 eV (0.0141) - 201 nm	HOMO→LUMO (99%)
		7.5958 eV (0.24039) - 163 nm	HOMO→LUMO+9 (97%)
<b>DO3S</b>	<b>A</b>	4.4605 eV (0.00689) - 278 nm	HOMO→LUMO (100%)
		5.31891 eV (0.02905) - 233 nm	HOMO-3→LUMO+4 (66%)
	<b>HA<sup>+</sup></b>	4.8827 eV (0.000354) - 254 nm	HOMO→LUMO (100%)
		5.98296 eV (0.02545) - 207 nm	HOMO-1→LUMO+10 (95%)
	<b>H<sub>2</sub>A<sup>2+</sup></b>	4.7593 eV (0.00220) - 260 nm	HOMO→LUMO (97%)
		6.05491 eV (0.07081) - 205 nm	HOMO-3→LUMO+3 (95%)
<b>DO4S</b>	<b>A</b>	4.3251 eV (0.00194) - 287 nm	HOMO→LUMO (100%)
		4.78384 eV (0.02606) - 259 nm	HOMO-2→LUMO+1 (61%)
	<b>HA<sup>+</sup></b>	4.8627 eV (0.000335) - 255 nm	HOMO→LUMO (98%)
		5.60689 eV (0.01931) - 221 nm	HOMO-5→LUMO+6 (100%)
	<b>H<sub>2</sub>A<sup>2+</sup></b>	4.7426 eV (0.00333) - 261 nm	HOMO→LUMO (100%)
		5.67375 eV (0.03349) - 219 nm	HOMO-4→LUMO (98%)

Table 9S. Values of pCd ( $= -\log[\text{Cd}^{2+}]$ ) at various pH for the complexes formed between  $\text{Cd}^{2+}$  and the given compounds ( $C_{\text{Cd}} = C_{\text{compound}} = 10^{-3} \text{ M}$ ). Values were computed from the speciation data, which for DO4S, DO3S and DO2A2S are reported in Tables 1 and 2, whereas for cyclen and DOTA were taken from references 54 and 62, respectively. For DO4S, DO3S and DO2A2S the reported pCd represent minimum values (see main paper).

<b>pH</b>	<b>DO4S</b>	<b>DO3S</b>	<b>DO2S2A</b>	<b>Cyclen</b>	<b>DOTA</b>
2	$\geq 4.8$	$\geq 3.9$	$\geq 3.9$	3.0	3.0
4	$\geq 6.8$	$\geq 5.9$	$\geq 6.2$	3.1	5.1
6	$\geq 8.7$	$\geq 7.9$	$\geq 8.2$	4.6	7.3
8	$\geq 10.4$	$\geq 9.6$	$\geq 10.2$	6.6	9.3



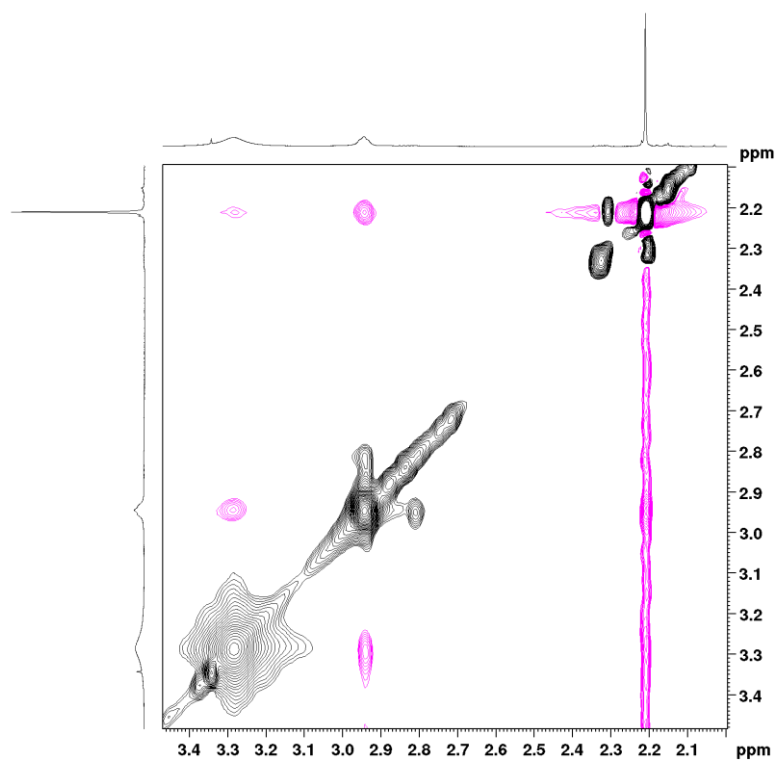


Figure 1S. NOESY spectrum of bis-protonated DO4S (solution at pD = 4.5, see Figure 3 in the main paper). The pink signals indicate spatial closeness, the grey ones indicate exchanging protons.

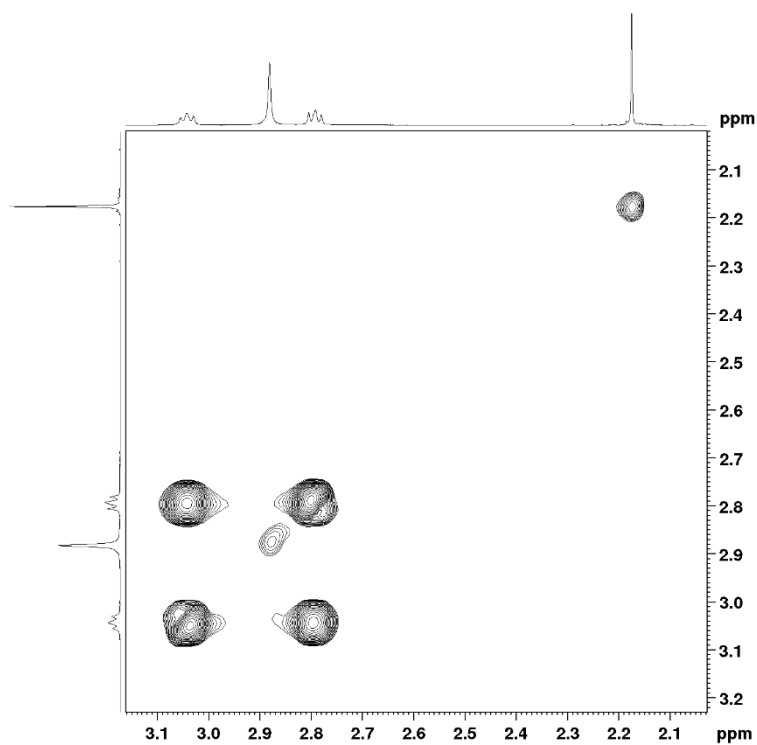


Figure 2S. COSY spectrum of monoprotonated DO4S (solution at pD = 9.8, see Figure 3 in the main paper).

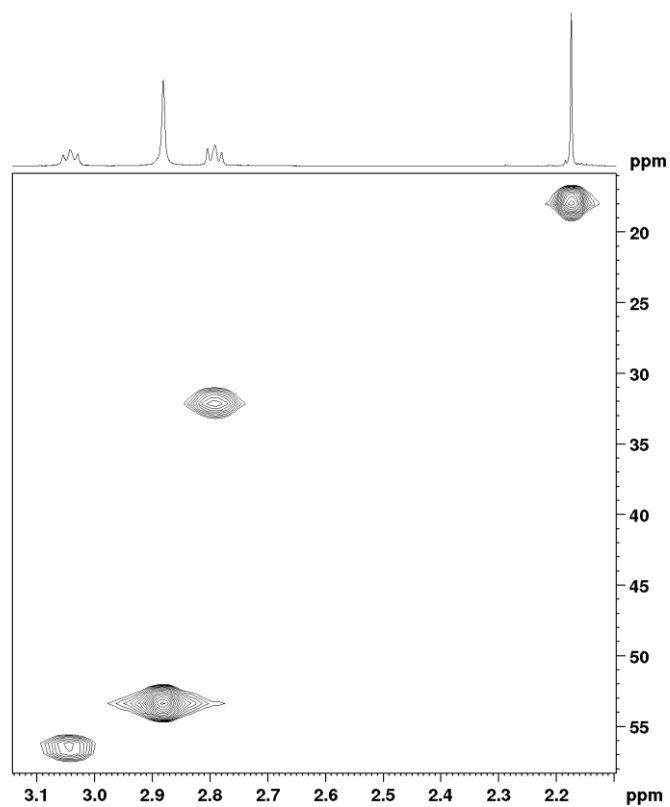


Figure 3S. HMQC spectrum of monoprotonated DO4S (solution at pD = 9.8, see Figure 3 in the main paper).

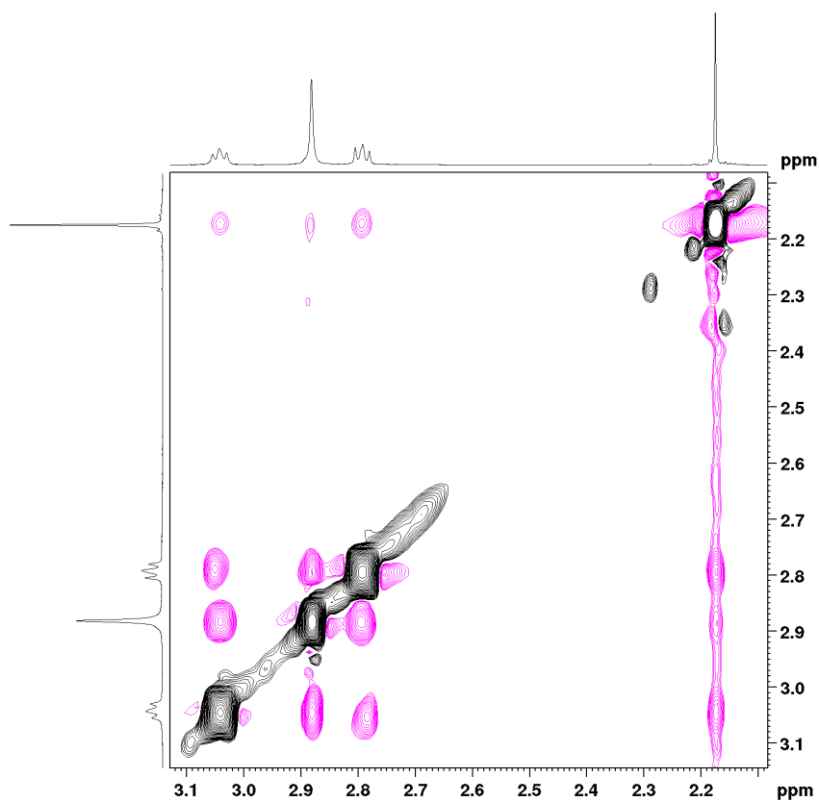


Figure 4S. NOESY spectrum of monoprotonated DO4S (solution at pD = 9.8, see Figure 3 in the main paper).

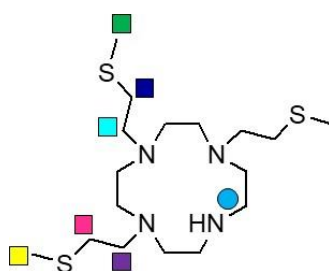
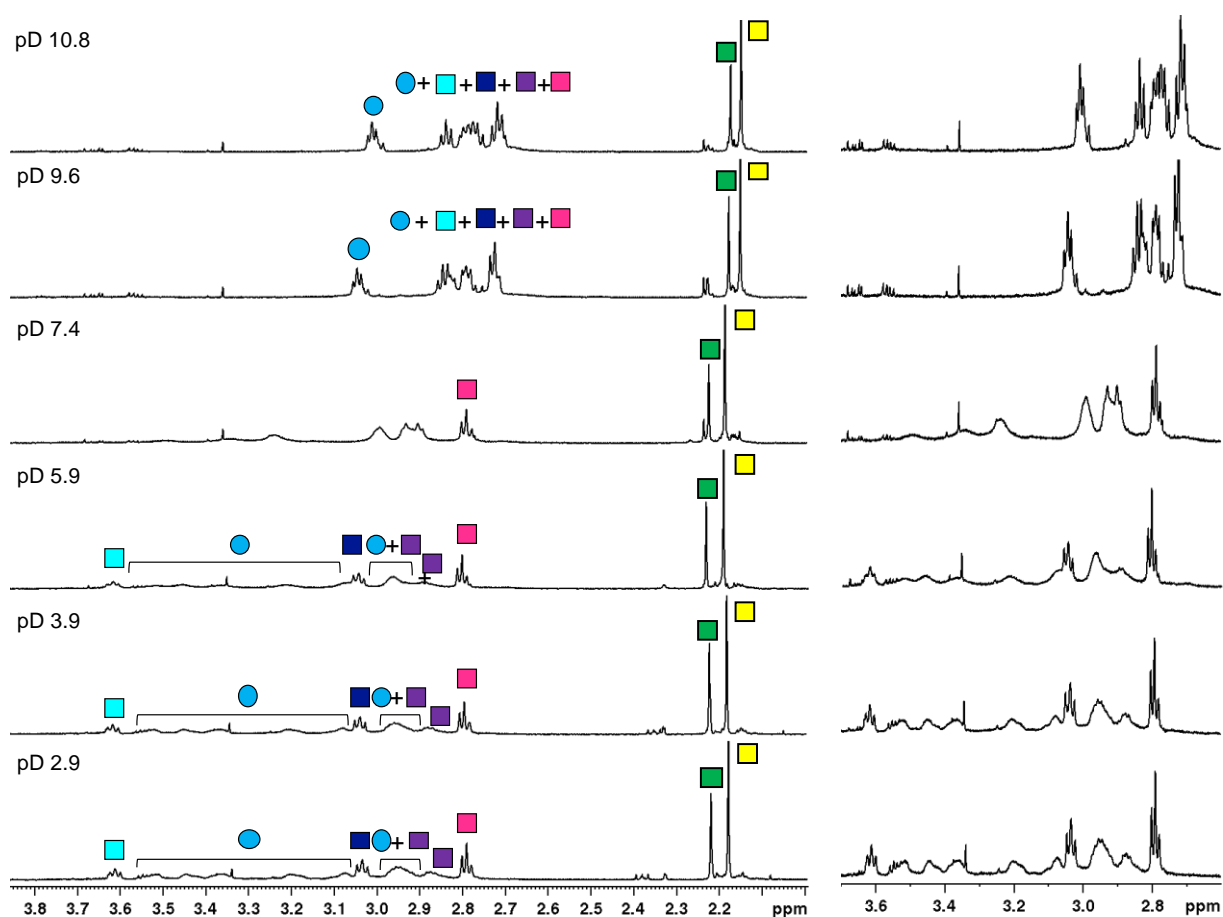


Figure 5S.  $^1\text{H-NMR}$  spectra of DO3S in  $\text{D}_2\text{O}$  at various pD values (total compound concentration:  $0.6 \cdot 10^{-3}$  mol/L). Left: full spectrum and signals assignment; right: enlargement of the ppm range 2.60-3.80. The signals at 2.30-2.40 ppm are produced by the internal reference, that at 3.35 ppm is due to residual methanol, and those at 3.60-3.70 ppm (at  $\text{pD} \geq 7.4$ ) are due to impurities.

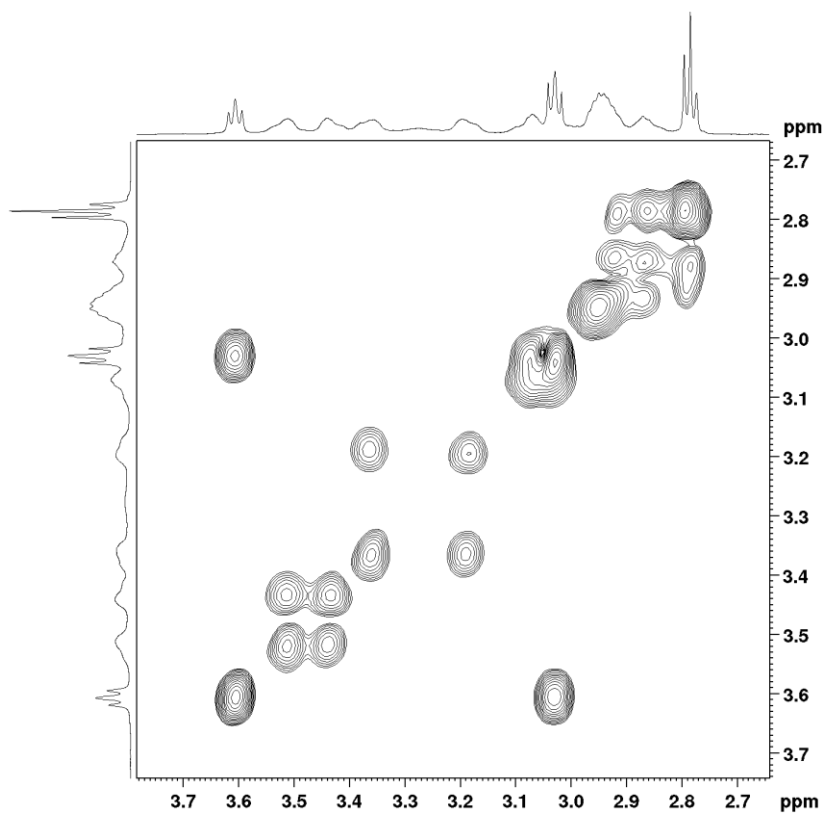


Figure 6S. COSY spectrum of bis-protonated DO3S (solution at pD = 3.9, see Figure 5S).

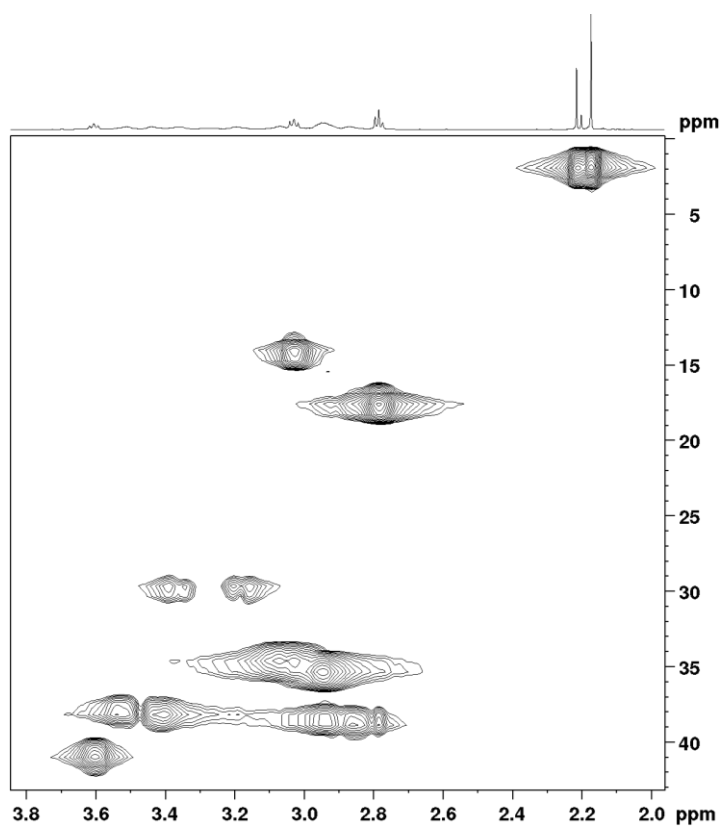


Figure 7S. HMQC spectrum of bis-protonated DO3S (solution at pD = 3.9, see Figure 5S).

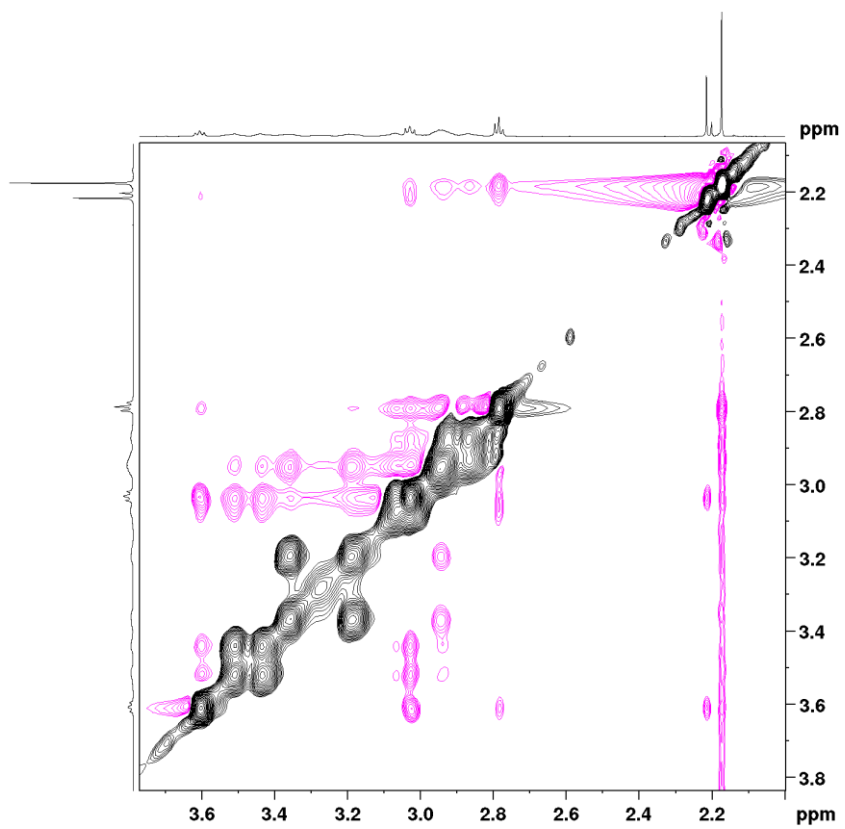


Figure 8S. NOESY spectrum of bis-protonated DO3S (solution at pD = 3.9, see Figure 5S).

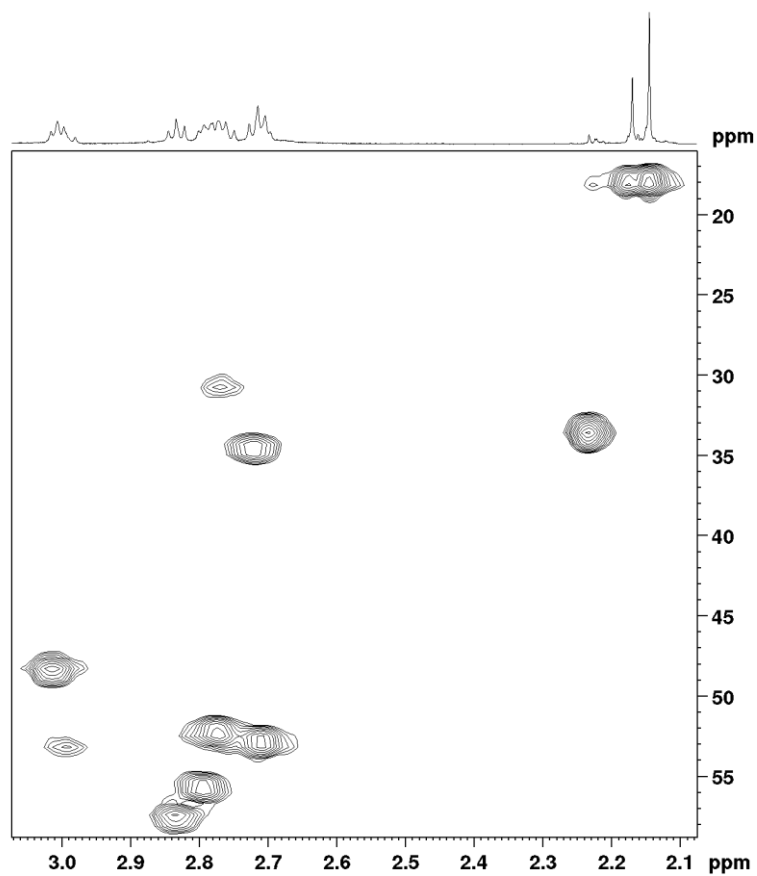


Figure 9S. HMQC spectrum of monoprotated DO3S (solution at pD = 10.8, see Figure 5S).

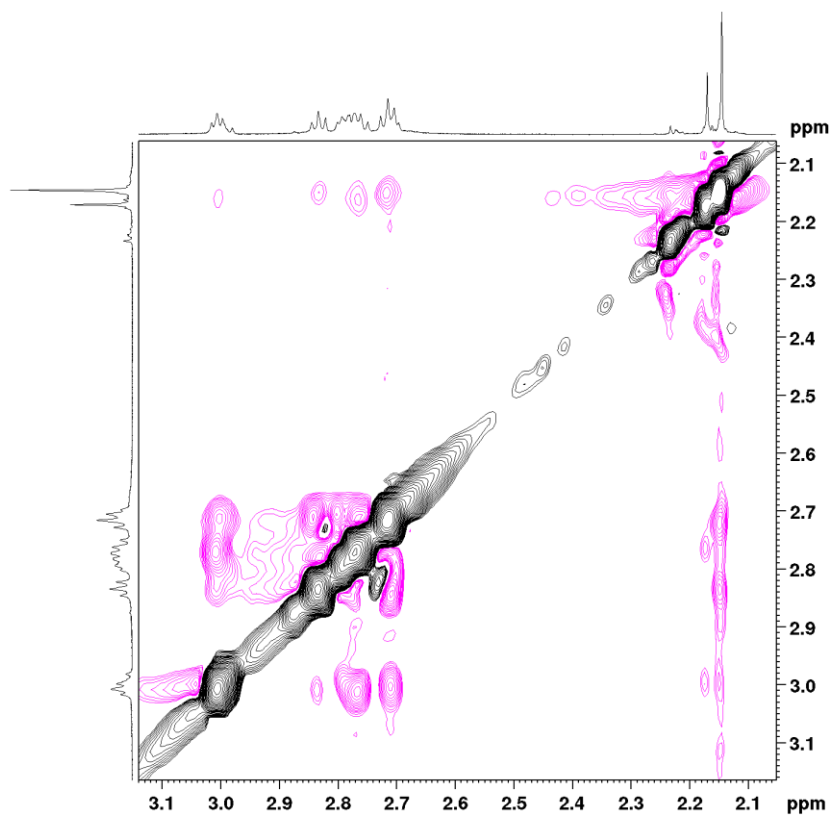


Figure 10S. NOESY spectrum of monoprotated DO3S (solution at pD = 10.8, see Figure 5S).

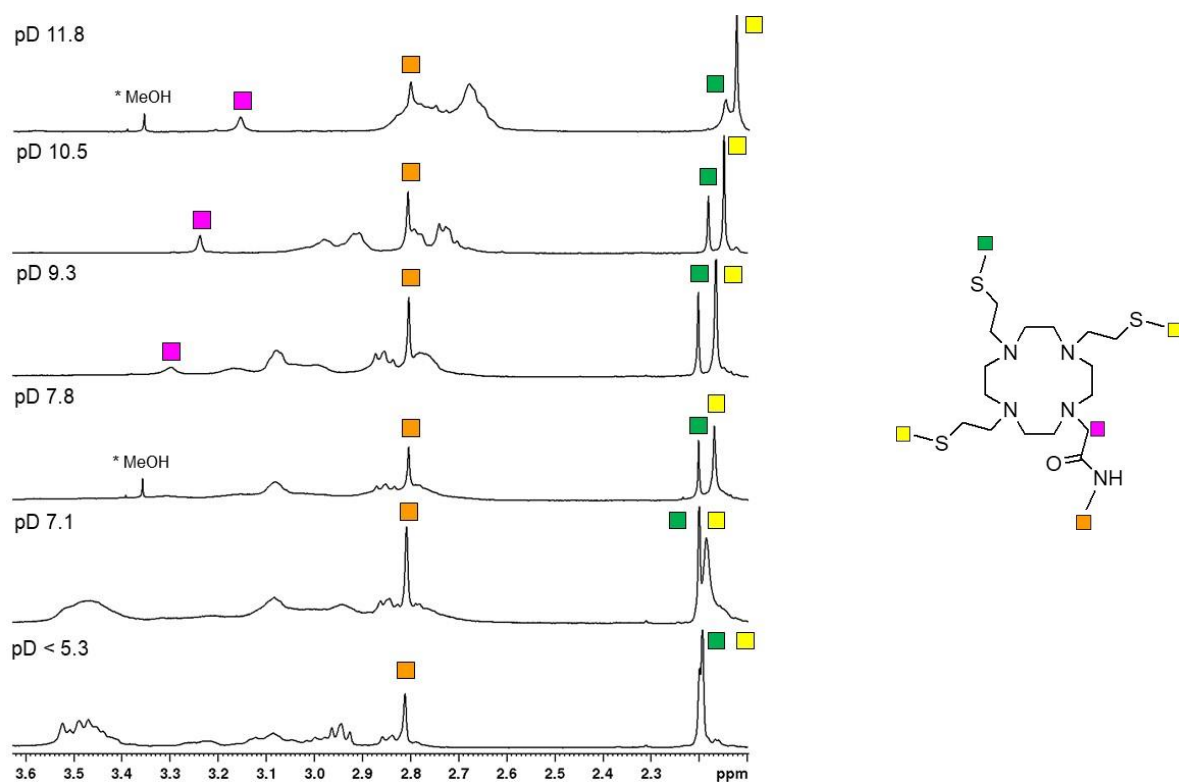


Figure 11S.  $^1\text{H-NMR}$  spectra of DO3SAm in  $\text{D}_2\text{O}$  at various pD values (total compound concentration:  $1.0 \cdot 10^{-3}$  mol/L). Left: full spectrum; right: signals assignment. Peak at 3.33 ppm is an impurity (residual methanol).

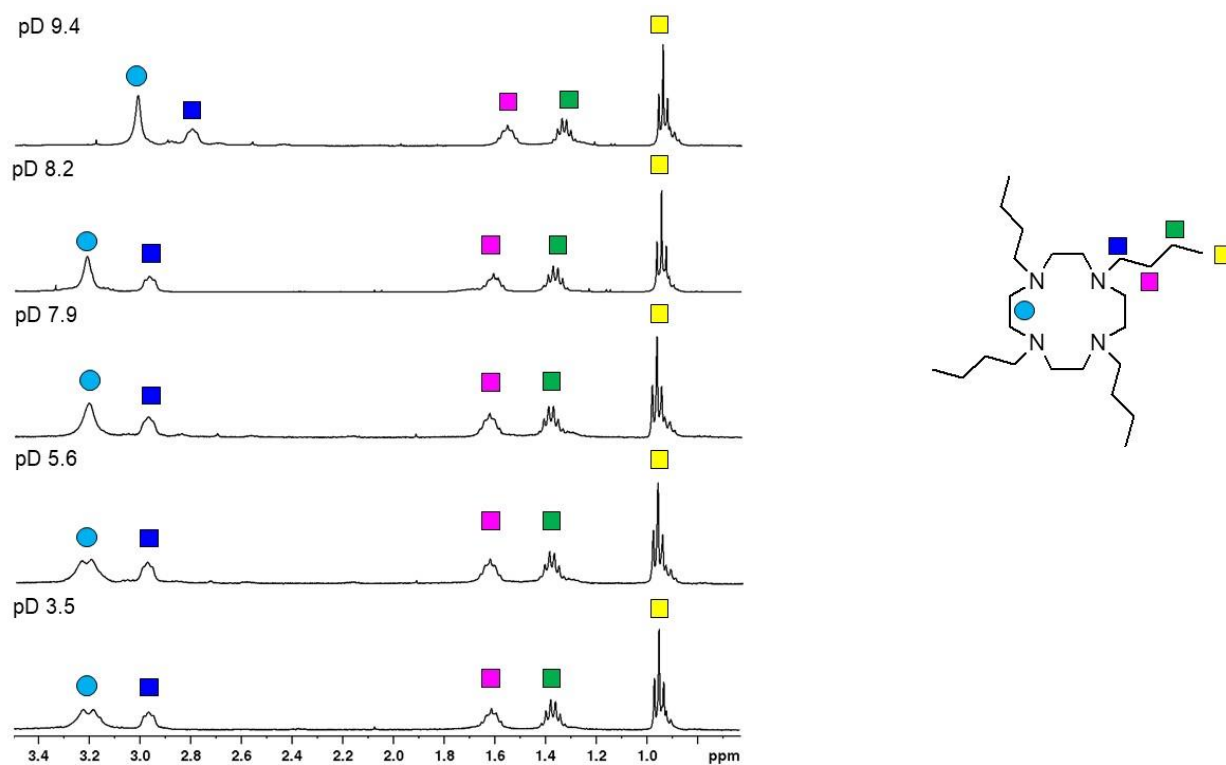


Figure 12S.  $^1\text{H-NMR}$  spectra of DOT-*n*-Bu in  $\text{D}_2\text{O}$  at various pD values (total compound concentration:  $0.8 \cdot 10^{-3}$  mol/L). Left: full spectrum; right: signals assignment.



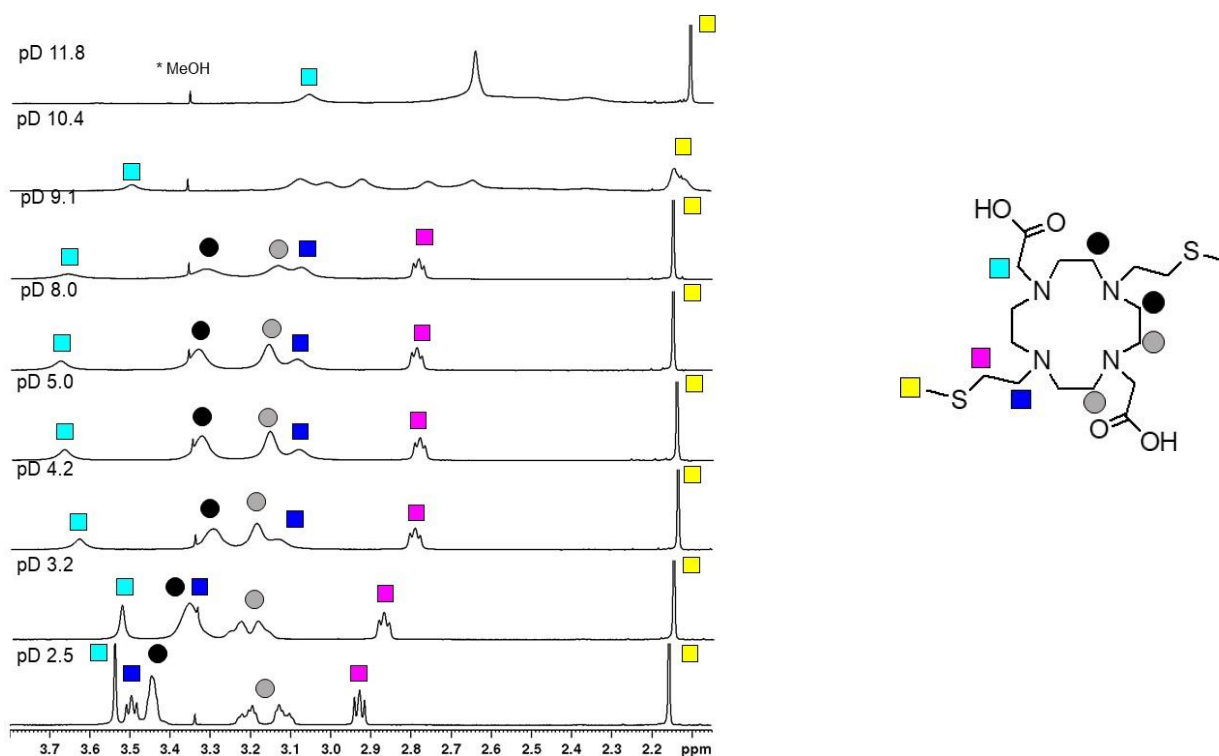


Figure 13S.  $^1\text{H-NMR}$  spectra of DO2A2S in  $\text{D}_2\text{O}$  at various pD values (total compound concentration:  $2 \cdot 10^{-3}$  mol/L). Left: full spectrum; right: signals assignment. Peak at 3.33 ppm is an impurity (residual methanol).

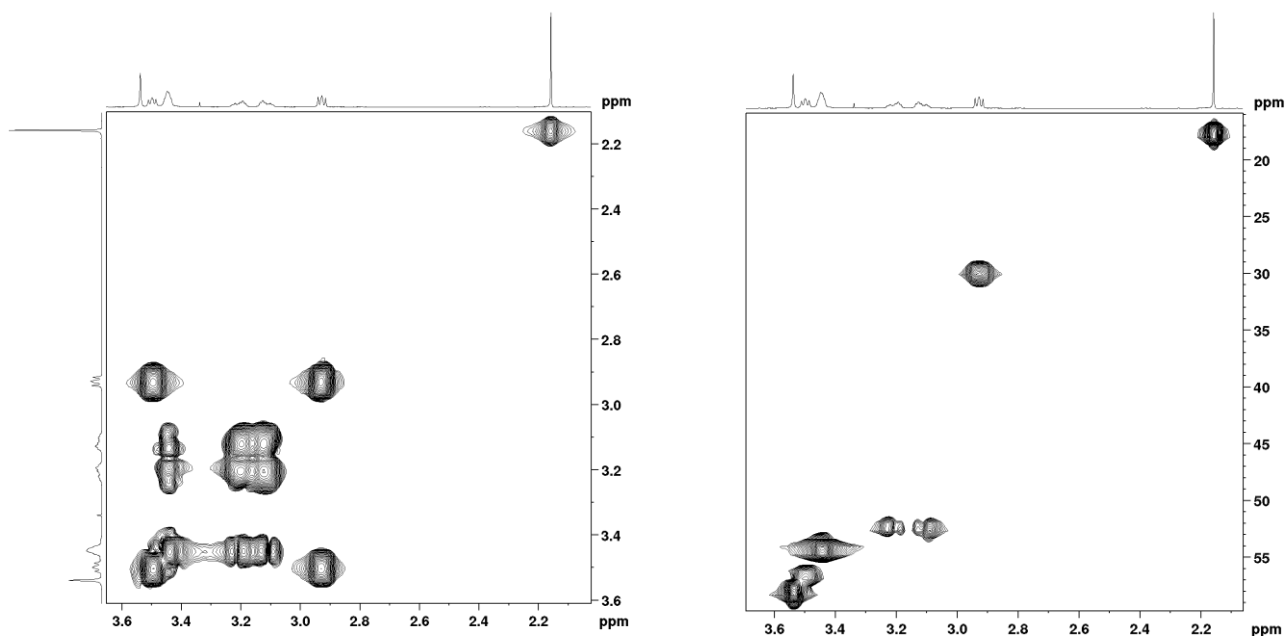


Figure 14S. COSY (left) and HMQC (right) spectra of the tris-protonated form of DO2A2S (solution at pD = 2.5, see Figure 14S).

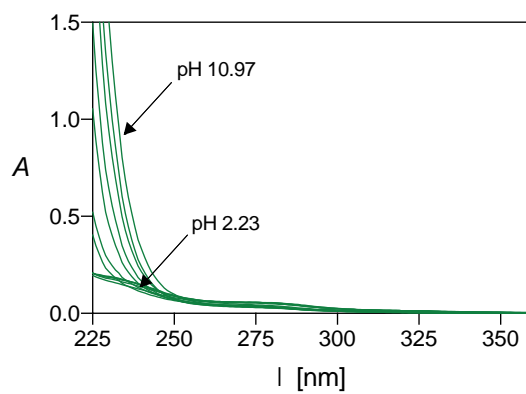


Figure 15S. UV-Vis spectra of solutions containing cyclen  $1.394 \cdot 10^{-2}$  mol/L. Spectra were obtained at pH values in the range *ca.* 2-11.

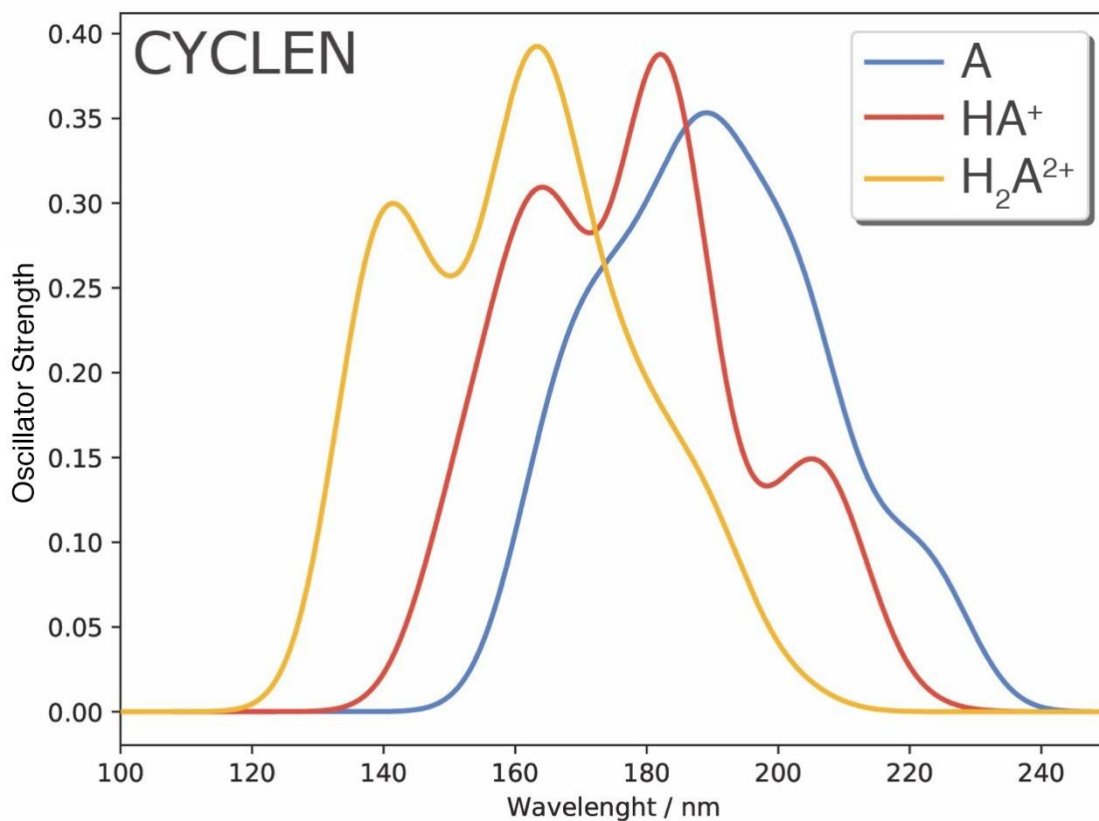


Figure 16S. Predicted UV/Vis spectrum (level of theory: COSMO-ZORA-SAOP/QZ4Pae//OPBE/DZP) for cyclen in three different protonation states.

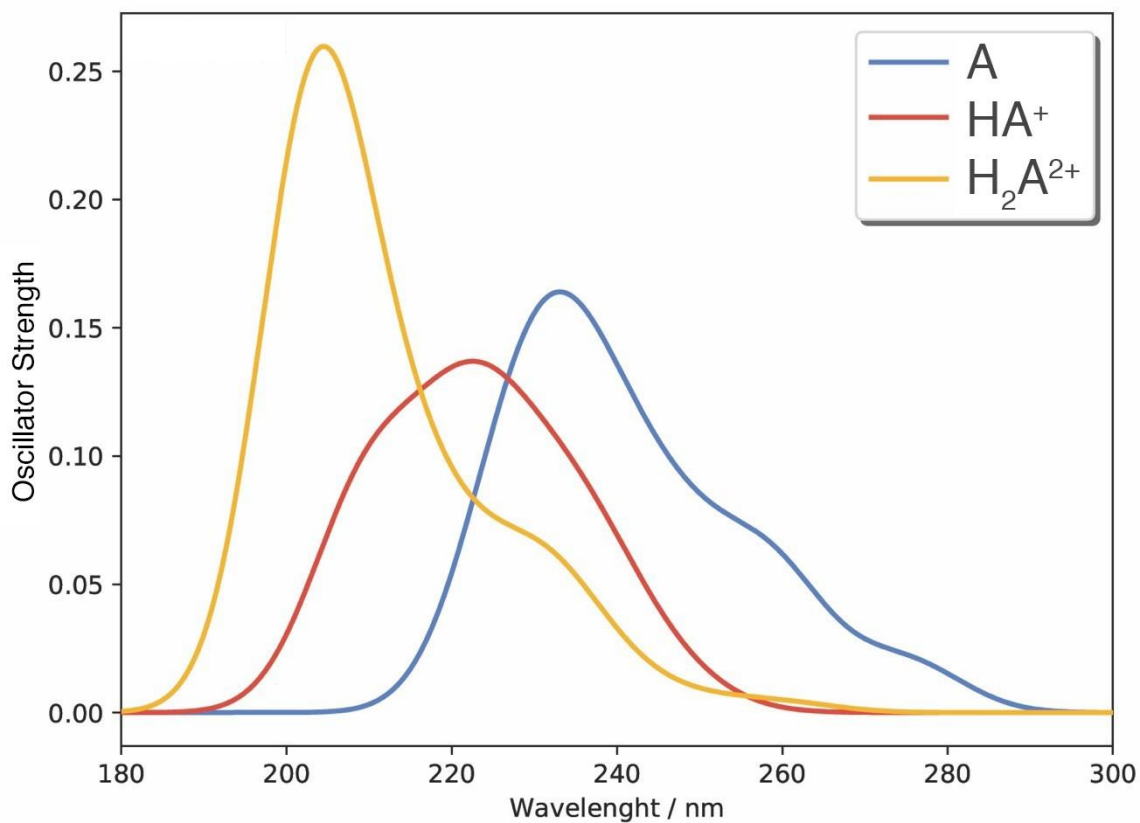


Figure 17S. Predicted UV/Vis spectrum (level of theory: COSMO-ZORA-SAOP/QZ4Pae//ZORA-OPBE/DZP) for DO3S in three different protonation states.

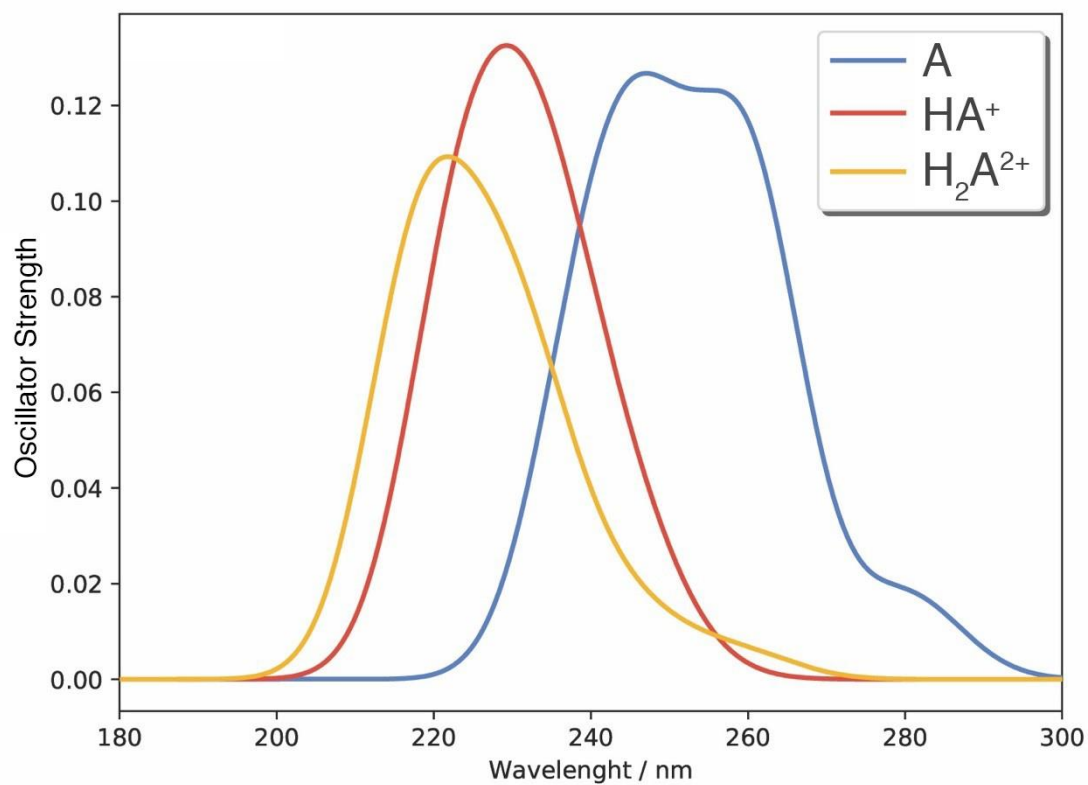


Figure 18S. Predicted UV/Vis spectrum (level of theory: COSMO-ZORA-SAOP/QZ4Pae//ZORA-OPBE/DZP) for DO4S in three different protonation states.

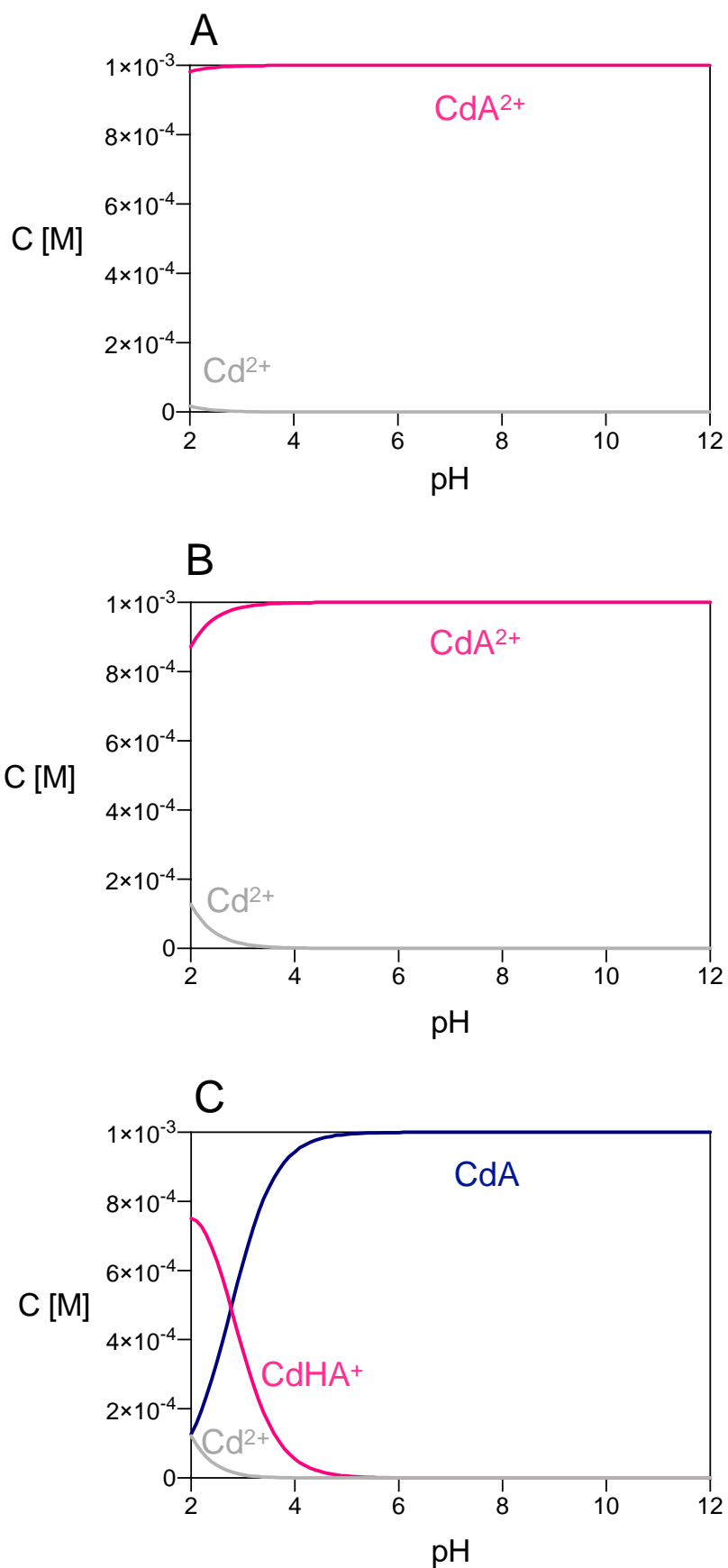


Figure 19S. Distribution diagrams of the  $\text{Cd}^{2+}$  complexes formed by A) DO4S, B) DO3S, C) DO2S2A ( $C_{\text{Cd}} = C_{\text{compound}} = 10^{-3}$  M,  $\text{NaNO}_3$  0.15 M, 25 °C). Diagrams were drawn considering the minimum stability constants values reported in Table 2 (main paper).

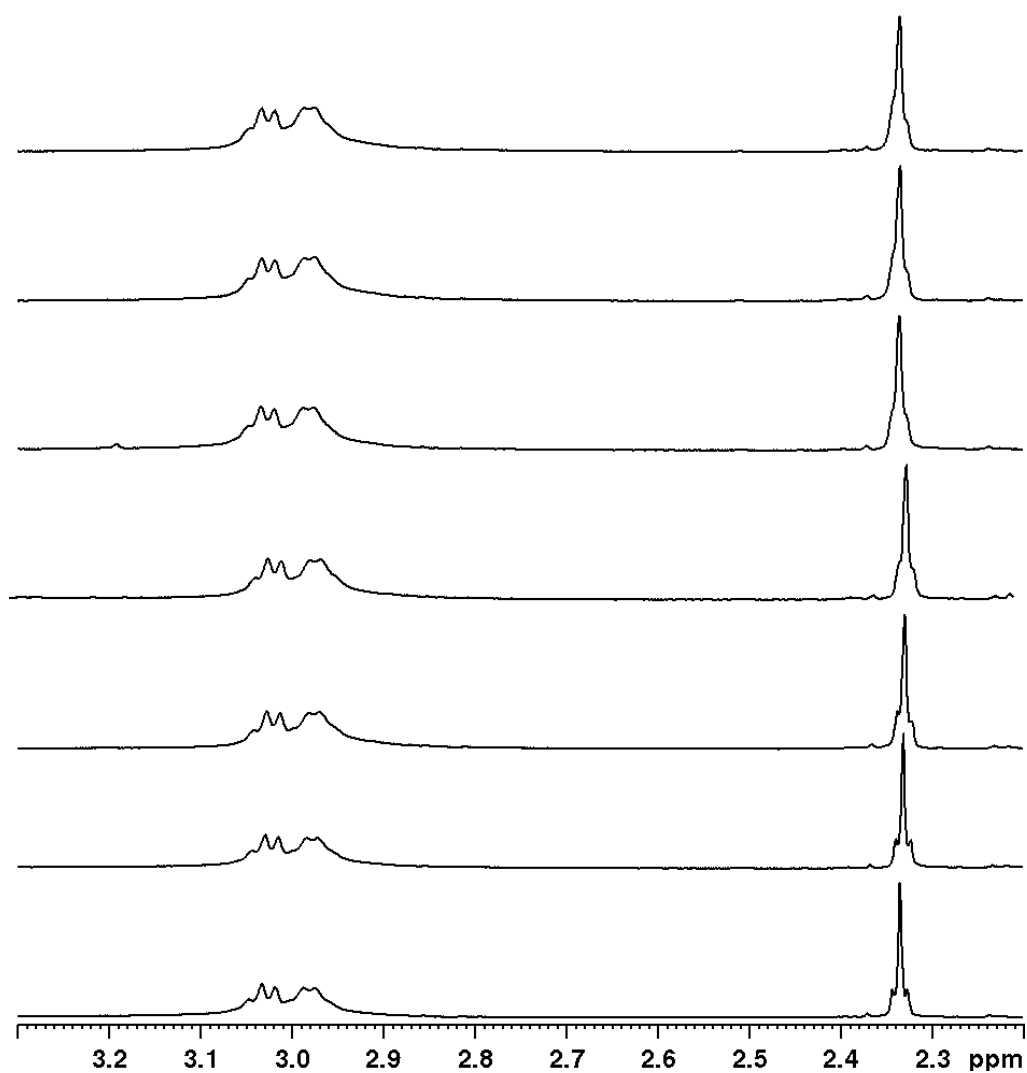


Figure 20S. <sup>1</sup>H NMR spectra of D<sub>2</sub>O solutions containing DO<sub>4</sub>S and Cd<sup>2+</sup> (400 MHz, D<sub>2</sub>O, C<sub>DO<sub>4</sub>S</sub> = 1.03·10<sup>-3</sup> M, C<sub>Cd</sub> = 1.06·10<sup>-3</sup> M) at various pD values. Based on the integration values, the singlet at 2.33 ppm (intensity = 12) was assigned to the terminal methyl (SCH<sub>3</sub>), whereas the multiplet centred at around 3.00 ppm (intensity = 32) was attributed to SCH<sub>2</sub> protons and to both ring and arms NCH<sub>2</sub> protons.

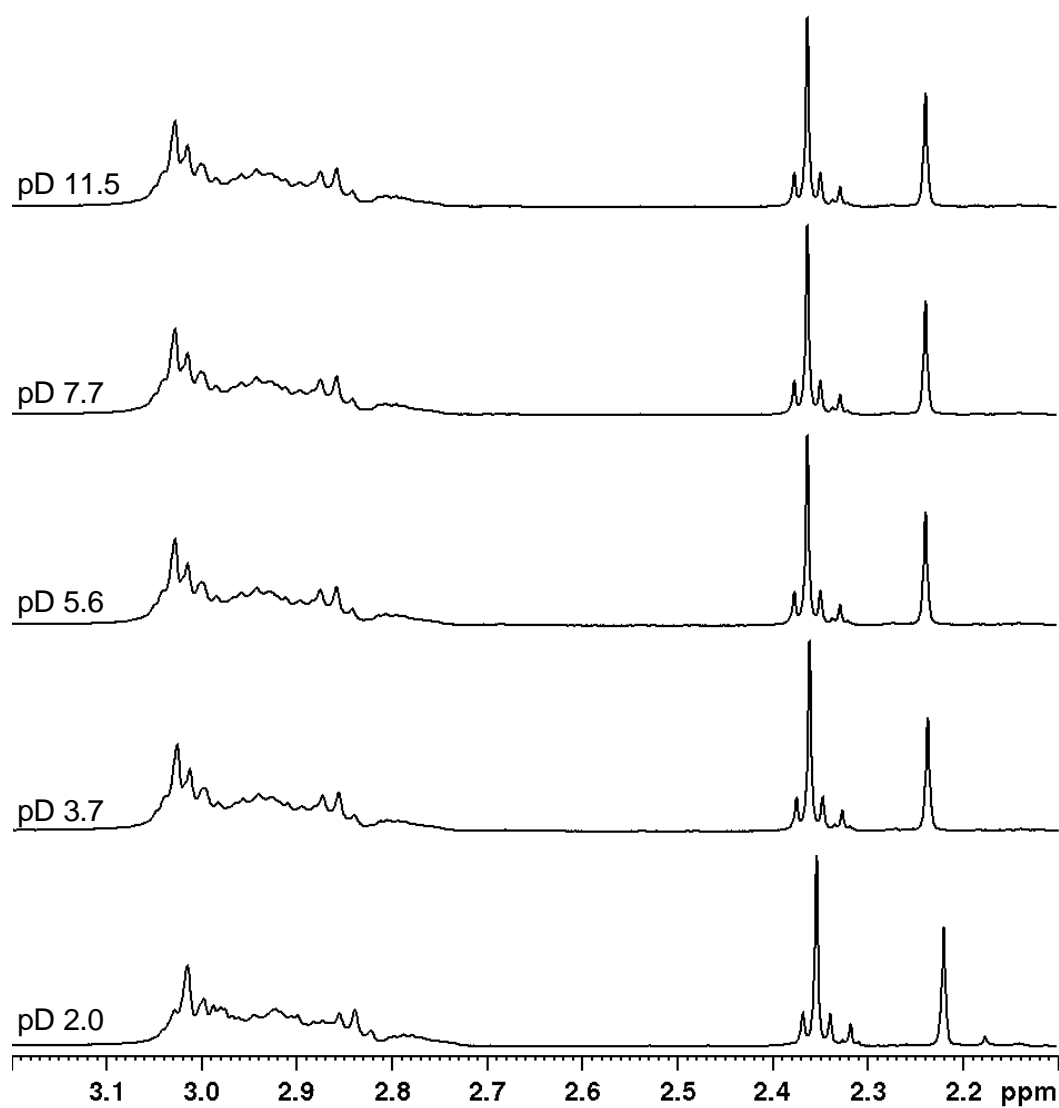


Figure 21S.  $^1\text{H}$  NMR spectra of  $\text{D}_2\text{O}$  solutions containing DO3S and  $\text{Cd}^{2+}$  (400 MHz,  $\text{D}_2\text{O}$ ,  $C_{\text{DO3S}} = 1.20 \cdot 10^{-3}$  M,  $C_{\text{Cd}} = 1.20 \cdot 10^{-3}$  M) at various pD values. Based on the integration values, the singlet at 2.21 ppm (intensity = 3) was assigned to the terminal methyl ( $\text{SCH}_3$ ) of the N4 side chain, whereas the singlet at 2.35 ppm (intensity = 6) was attributed to  $\text{SCH}_3$  protons of the N1 and N7 side chains. The multiplet centred around 2.80-3.00 ppm (intensity = 28) was attributed to  $\text{SCH}_2$  protons and both ring and arms  $\text{NCH}_2$  protons.

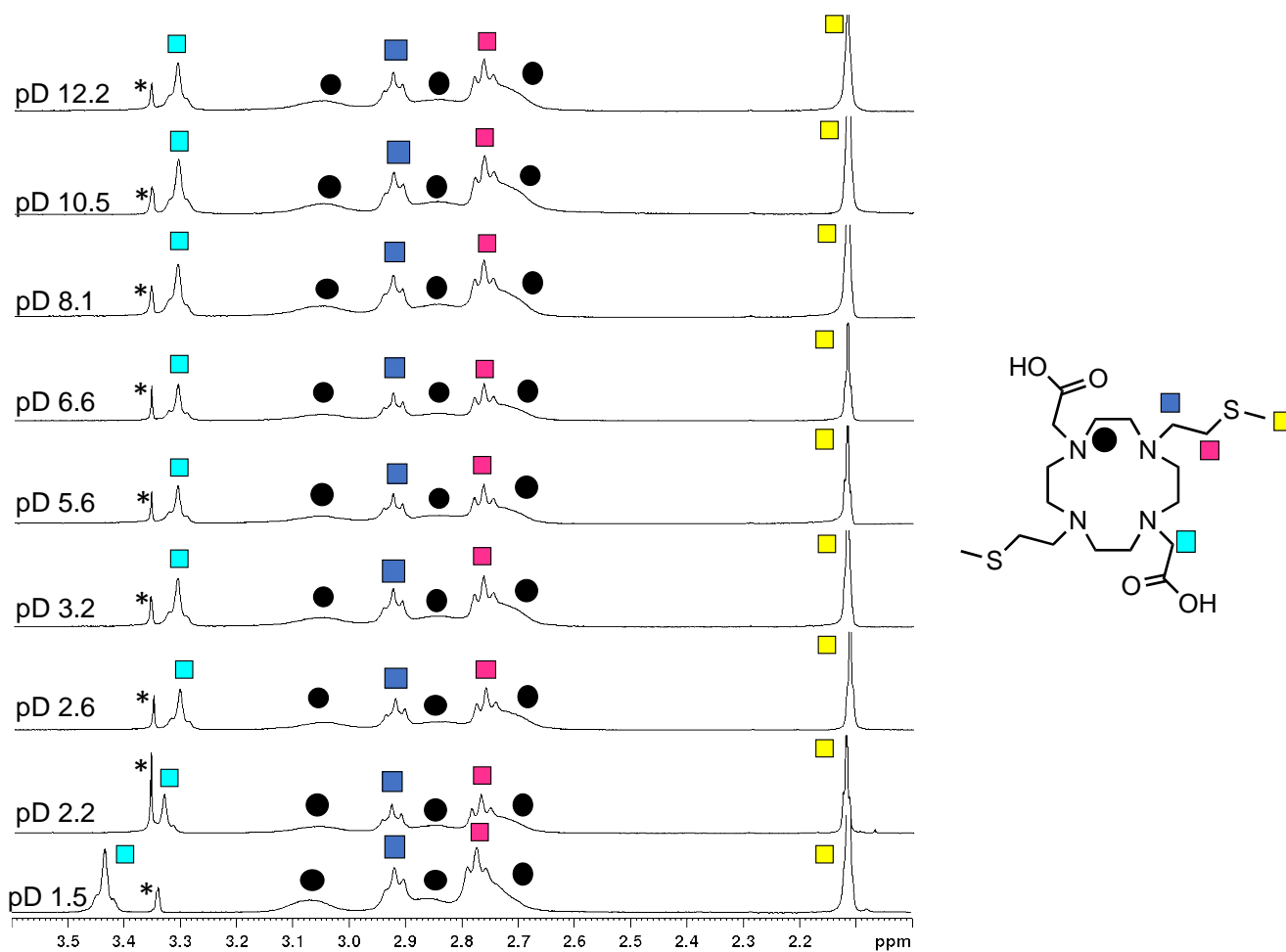


Figure 22S.  $^1\text{H}$  NMR spectra of  $\text{D}_2\text{O}$  solutions containing DO2A2S and  $\text{Cd}^{2+}$  (400 MHz,  $\text{D}_2\text{O}$ ,  $C_{\text{DO2A2S}} = 1.30 \cdot 10^{-3}$  M,  $C_{\text{Cd}} = 1.30 \cdot 10^{-3}$  M) at various pD values. The signals marked with an asterisk are related to MeOH impurities. Proton assignment is reported on the right and it was based on integration values and on the similarities with the spectra of the free ligand (Figure 13S).